

Grading method for tomato multi-view shape using machine vision

Liping Chen^{1,4}, Tingting He^{1,2}, Zhiwei Li², Wengang Zheng^{3,4}, Shunwei An⁵, Lili ZhangZhong^{1,4*}

(1. Intelligent Equipment Technology Research Center, Beijing Academy of Agriculture and Forestry Sciences, Beijing 100097, China;

2. Shanxi Agricultural University, Taigu 030801, Shanxi, China;

3. Information Technology Research Center, Beijing Academy of Agriculture and Forestry Sciences, Beijing 100097, China;

4. Agricultural Information Software and Hardware Product Quality of the Ministry of Agriculture Key Laboratory of Testing, Beijing 100097, China;

5. Beijing Agricultural Extension Station, Beijing 100097, China)

Abstract: Owing to the requirements of a high yield and high-quality tomatoes, tomato grading is important-particularly for fruit morphology, and accuracy has become the focus of attention. Machine vision provides a fast and nondestructive manner to address this demand. In this study, the gamma correction method was used for preprocessing to enhance the edge information of tomatoes, and Otsu's method was used to eliminate the tomato-image background in the A-component image under the LAB color model. On this basis, two levels of exploration were conducted. First, new evaluation indices were proposed for tomato shapes from different views. For the top view, two shape-evaluation indices were established: the area ratio of the maximum inscribed circle to the maximum circumscribed circle and the dispersion of the contour centroid distance (range and coefficient of variation), the highest accuracy was 94%. For the side view, the difference between the maximum and minimum centroid distances in the contour was established as a shape index, the highest accuracy was 91.91%. Second, an evaluation method based on multi-view fusion was developed by combining the advantage indices for different views. The classification accuracy reached 96%, with the highest identification accuracy of unqualified tomatoes. The results show that the proposed evaluation method combining top views (dispersion of centroid distance) with side views (difference between maximum and minimum centroid distances) is effective for classifying tomatoes.

Keywords: machine vision, centroid distance, multi-view, tomato shape, grading method

DOI: [10.25165/j.ijabe.20231606.7768](https://doi.org/10.25165/j.ijabe.20231606.7768)

Citation: Chen L P, He T T, Li Z W, Zheng W G, An S W, ZhangZhong L L. Grading method for tomato multi-view shape using machine vision. *Int J Agric & Biol Eng*, 2023; 16(6): 184–196.

1 Introduction

Tomato is one of the three world-traded vegetables and occupies an important position in the global vegetable trade. China is the country with the largest tomato production and export volume in the world. In 2020, China produced 65.15 million t of tomatoes, accounting for almost one-third of the global tomato production^[1]. Tomato quality is a key factor that affects tomato export and sales volume. According to the national standard “Grades and specifications of tomatoes”^[2], the grade evaluation indicators for tomato quality include shape, color, and surface damage, and the grading requirements for fruit shape indicate that the fruit must be round without ribs and not deformed. At present, the detection of tomato shapes is mainly based on visual inspection or mechanical sorting. These methods are highly subjective, time-consuming, and labor-intensive, and they can easily cause contamination or damage to the tomato surface^[3]. Therefore, it is imperative to develop an

efficient and accurate nondestructive testing method for tomato shape detection.

The emergence of machine vision technology has provided a new approach to the non-destructive grading of agricultural products. The detection technology of appearance properties such as maturity^[4,5], shape^[6,7], and surface defects^[8,9] of agricultural products based on machine vision typically includes four steps: image acquisition, image processing, feature extraction, and classification. Among these, the extraction and selection of features is a key step that affects the accuracy of classification. The features used for tomato shape discrimination in previous studies mainly included the ratio of the maximum longitudinal diameter to the maximum transverse diameter, circularity, and Fourier descriptor^[10]. Cai^[11] compared the accuracy and practicability of tomato shape classification using the ratio of the maximum longitudinal diameter to the maximum transverse diameter, the circularity, and the Fourier descriptor and used the circularity feature to achieve the classification of tomato shape. Wang^[12] used the circularity and the ratio of the maximum longitudinal diameter to the maximum transverse diameter as the shape characteristics to identify the tomato. Arjenaki et al.^[13] extracted the lengths of the long and short axes of the tomato to calculate the eccentricity for measuring the circularity of the tomato. The detection method based on the roundness and the maximum ratio of the longitudinal diameter to the transverse diameter is relatively accurate, but its classification accuracy is overly dependent on the angle of image acquisition. Thus, scholars have proposed the use of features with scale and rotation invariance i.e., Fourier descriptors^[14] and image moments

Received date: 2022-06-29 **Accepted date:** 2023-03-07

Biographies: Liping Chen, PhD, Researcher, research interest: precision agriculture, Email: chenlp@nercita.org.cn; Tingting He, MS, research interest: agricultural engineering, Email: baymaxhtt159@foxmail.com; Zhiwei Li, Professor, research interest: agricultural informatization, Email: lizhiweitong@163.com; Wengang Zheng, PhD, research interest: agricultural information, intelligent equipment technology, Email: zhengwg@nercita.org.cn; Shunwei An, Senior Agronomist, research interest: vegetable water and fertilizer integration technology, Email: shunwei112@163.com.

***Corresponding author:** Lili ZhangZhong, PhD, Associate Researcher, research interest: agricultural informatization water saving technology, Email: lilizhangzhong@163.com.

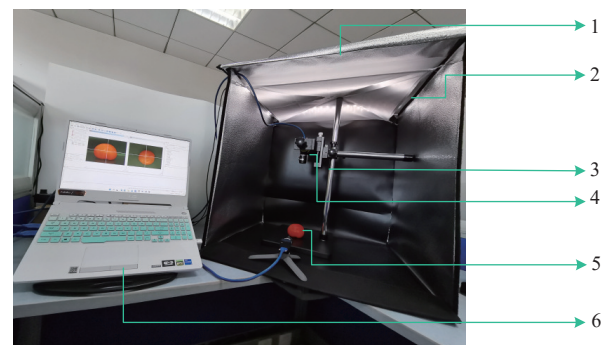
such as Hu moment^[15], Zernike moment^[16,17], wavelet moment^[18], that describe the tomato contour. Li et al.^[19] used Fourier descriptors to extract shapes from tomato depth images for shape classification, with an average classification accuracy of 92%. Wang and Mu^[15] used the Hu moment as a feature parameter and used support vector machines to classify tomato shapes. Yuan et al.^[20] and Liu et al.^[21] used the first-order Fourier descriptor of tomato contours to characterize the shapes of target tomatoes, the classification accuracies were 90.0% and 91.1%, respectively. Yao et al.^[22] calculated the Fourier descriptor of the octagonal contour after the transformation of contour coordinates into polar coordinates, and recognized the corner lobe shape of the octagonal contour. In addition, Fourier descriptors have also been successfully applied to crops such as almonds^[23], strawberries^[24], and roses^[25]. The shape-detection methods based on the Fourier descriptor and image moment overcome the misidentification caused by the image acquisition angle to a certain extent; however, their calculation method was complex. In recent years, some scholars have exploited the variation characteristics of the contour curve of the fruit and designed shape-detection indicators based on fruit-specific contour characteristics to increase classification accuracy. For example, the boundary coordinates of red dates were converted into polar coordinates, and curve fitting was performed; then, normal and deformed jujubes were classified according to the minimum radius difference in the polar coordinate system^[26]. Additionally, a method for detecting abnormal cherries according to the shape of the Euclidean distance curve from the cherry pedicle to a boundary point was proposed^[27]. For grapefruit, the rectangular coordinates of the grapefruit contour are converted into polar coordinates and the contour curve was fitted; then, the values of the peaks and troughs of the fitting curve were extracted to discriminate the grapefruit shape^[28]. The shape-detection method based on the fruit contour curve has a higher precision and detection efficiency than methods such as circularity and Fourier descriptors. At present, this method based on the appearance contour curve has a very good effect on the evaluation of the transverse shape of fruits with obvious shape characteristics, such as dates, and grapefruit^[29]. The difficulty of using machine-vision technology to detect the tomato shape was that different varieties of tomatoes have different shape characteristics. For tomatoes of the same variety with different shapes, the differences between adjacent shape levels were vague, and the discriminant result has a strong correlation with the image-acquisition angle, leading to considerable difficulty in the detection of the tomato shape. In conclusion, the detection of tomato shapes can be theoretically realized by detecting the special change trend of its fruit shape contour curve.

The technology for nondestructive inspection of fruit and vegetable shapes using machine vision is mature. Current research on tomato shape identification is limited to the analysis of the top-view image; however, the description of the tomato shape in the actual production and packaging process should also include the side shape. Therefore, in this study, the tomato—a typical grading product—was taken as the research object, a dual-view image-acquisition system was used to obtain top- and side-view images of tomatoes, and an analysis was performed using machine-vision technology based on the change characteristics of the tomato contour curve. The main research goals were as follows: 1) to propose new indicators for tomato shape evaluation via top and side views, and to optimize and screen them; 2) to develop a multi-view fusion tomato shape evaluation framework and analysis method for high-precision and non-destructive online grading of tomatoes.

2 Materials and methods

2.1 Image acquisition

The tomato variety used in the experiment was Cappricia, and its shape was round. Tomato images were collected from July to November 2021, and 300 tomatoes were selected as experimental samples (200 tomatoes were used to determine the classification threshold, and 100 tomatoes were used for validation). The image-acquisition system, shown in Figure 1, employed a small studio with a size of 65×65×65 cm³ as the basic frame, which included three modules: light source, imaging, and data transmission. The light-source module was composed of two rotatable light panels (5500 K, 12 V) inlaid with high-brightness light-emitting diode lamp beads and a soft cloth (1.2×1.0 m²), which satisfied the lighting requirements of multi-directional and multi-brightness fill light and reduced the reflective area of the tomato surface to a certain extent. The imaging module included an MER-500-14U3C-L color camera (Daheng Mercury series) with 5 million pixels, a resolution of 2592×1944, and a 12-mm-focal length OPT-C1214-2M fixed-focus lens. Considering the cost, the experiment only installed two sets of imaging equipment above and in front of the studio to obtain images of the top, bottom, and side of tomatoes, with a shooting distance of 300 mm. It should be noted that the camera used to collect the tomato side view image acquires the image through the small window in the front of the studio, which can effectively avoid the impact of external ambient light on image acquisition. The transmission of the image data was realized by a high-flex line with model U3 Micro-B/S to A. The collected photographs were saved on a computer in the “.jpg” format, and at least four images were collected for each tomato. Figure 2 shows top and side views of tomatoes with different shapes.



1. Background frame 2. Light source 3. Camera stand 4. Camera and lens 5. Tomato sample 6. Computer

Figure 1 Image-acquisition studio

2.2 Image processing

2.2.1 Image preprocessing

Because the tomato surface is prone to surface reflection, the illumination cannot be excessively strong during image acquisition; however, under weak illumination, the boundary information of the tomato cannot be clearly obtained (Figure 3a). Therefore, on the premise of ensuring a small surface reflection area, the gamma transform algorithm was used to increase the brightness of the image boundary. The gamma transform can correct bleached (camera-overexposed) pictures or pictures that are too dark (underexposed). Gamma transform can increase image contrast while image enhancement, making the difference between tomato target and background pixel more obvious. In this study, several popular image enhancement algorithms were used to test, and finally, the gamma change with the best effect was selected to

complete the brightness enhancement of tomato images. It is expressed as follows:

$$s = cr^\gamma \tag{1}$$

where, r represents the gray value of the image to be enhanced; s represents the gray value of the image after enhancement; c is a constant; the exponent γ determines the effect of the image enhancement. When $\gamma > 1$, the gray level of the bright area is stretched, and the gray level of the region is compressed to a darker level; that is, the overall image becomes darker. When $\gamma < 1$, the

opposite effect is observed. In this study, $\gamma = 0.5$ was selected for image enhancement, and an example is shown in Figure 3b. It can be seen that in the tomato image after gamma transformation, the contour information of the tomato was more obvious than in the original image, meanwhile, the salt-and-pepper noise generated during imaging and transmission became more obvious. The median filter has a good filtering effect on salt and pepper noise, which can maintain the edge characteristics of the image and will not cause significant blur. Therefore, the median-filter algorithm was used to denoise the images after image enhancement (Figure 3c).

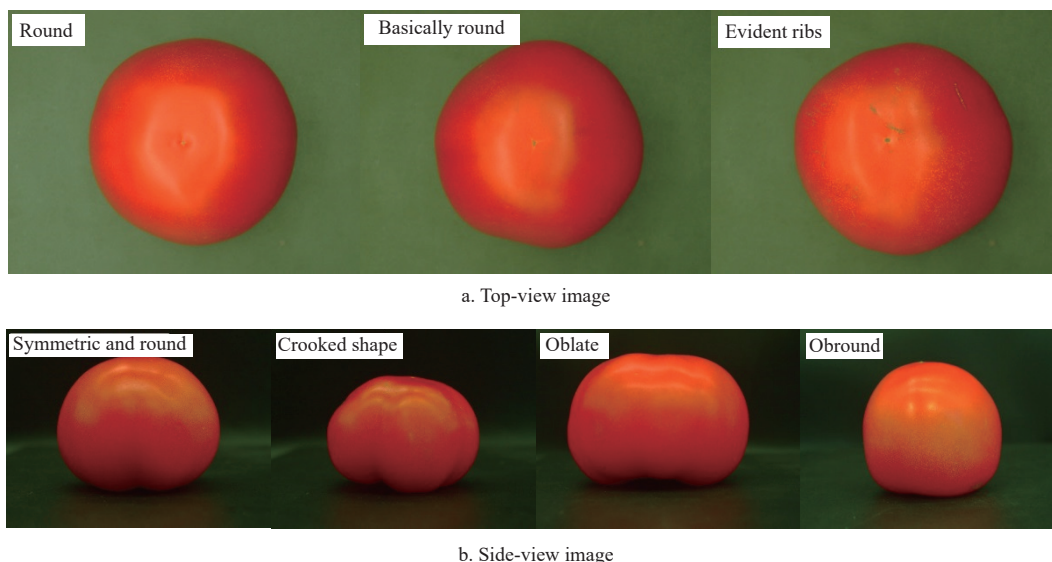


Figure 2 Tomato images from different views

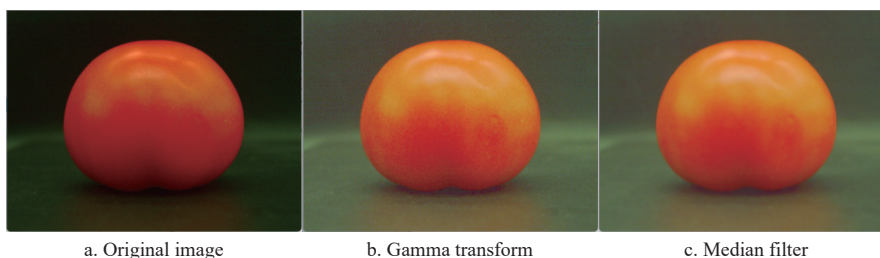
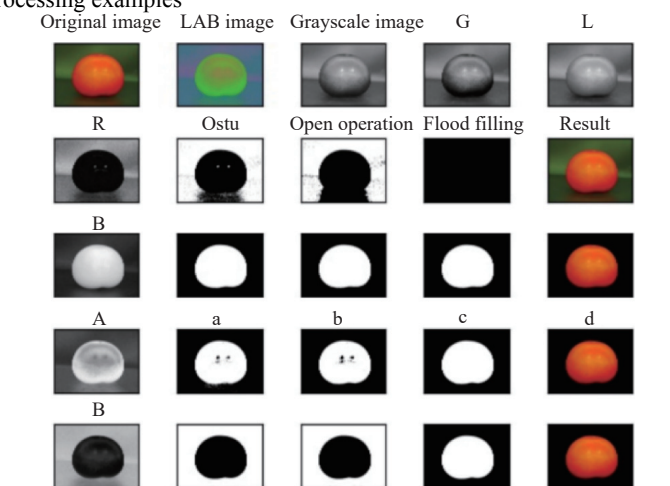


Figure 3 Image preprocessing examples

2.2.2 Image segmentation

When the sample images were collected, the interior of the studio was covered with black light-absorbing paper; thus, each collected tomato image had a single background, and the difference between the tomato target and the background pixels was evident. In this event, the tomato target and background could be quickly segmented via Otsu's threshold-segmentation method. To facilitate the separation of the target and the background in the image, the tomato image of each component in the red-green-blue (RGB) and LAB color models was extracted, as shown in Figure 4. Under the lighting conditions used in this study, the colors of the target and the background in the grayscale image were similar, and they were difficult to distinguish, whereas the foreground and background could be clearly distinguished in the R and B components in the RGB color model and the A and B components in the LAB color model. The R, B, A, and B component images were used for segmentation, and the A-component image exhibited the best segmentation effect. In the other component images, the background was not completely removed (R-component), or the



Note: R represent R-component in RGB; The third line B represent B-component in RGB; A represent A-component in LAB; The five line B represent B-component in LAB; G represent G-component; L represent L-component; a, b, c, d as a serial number identifier, representing the graph below.

Figure 4 Image segmentation of tomatoes

edge of the tomato fruit was missing (B-component in RGB and LAB color model). Therefore, the A-component diagram of the tomato was selected for image segmentation. During threshold segmentation, some small highlighted areas on the tomato surface (not the edge part) were mistakenly segmented as the background (Figure 4a), and the image was processed using the morphological open operation to eliminate these small areas while trimming the image edge burrs (Figure 4b). Then, the flood-filling algorithm was used to fill those larger-area holes that could not be eliminated by the open operation (Figure 4c). Finally, the filled binary image was added to the original image to obtain the tomato image with the background removed (Figure 4d).

2.3 Shape-detection process

The key steps in tomato shape detection based on machine vision are feature extraction and shape discrimination. According to the national classification standard for tomato shape in “Grades and specifications of tomatoes” and the Beijing local standard “Identification experiment code for vegetable varieties Part 1: Solanaceous fruits”^[30], detection methods based on the shape characteristics of the tomato top view and side view, respectively, were developed.

Top view: The area ratio of the maximum inscribed circle to the maximum circumscribed circle and the dispersion of the tomato centroid distance were defined as new indicators for detecting the tomato shape. Common shape features such as the roundness, fitting degree of the minimum circumscribed circle, the ratio of the maximum longitudinal diameter to the maximum transverse diameter, and eccentricity were extracted for comparison, and the characteristic indicators suitable for tomato top-view shape detection were selected. **Side view:** The height difference between the two adjacent peaks and the height difference between the minimum wave trough and its adjacent peaks of the centroid distance curve were defined to detect the symmetry and the oblong-oblate degree; two frequently-used features, (the ratio of the longitudinal diameter to the transverse diameter and the fitting degree of the minimum circumscribed circle of the contour) were extracted as controls to identify the feature indices suitable for the shape detection of the tomato-side view. The judgment results of three experts with years of experience in tomato quality sorting on tomato shapes are used as the true labels of the samples to evaluate the accuracy of the shape grading method for top and side-views. The accuracy of shape classification was evaluated by calculating the percentage of samples that were correctly classified, and the multi-view shape judgment results were integrated to obtain the overall shape grade of the tomato.

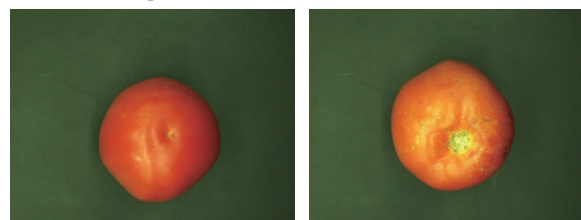
2.4 Work platform

The experimental work platform included two parts: hardware and software. The hardware was configured with an Intel Core i5-11400h CPU, 16.0 GB of random-access memory, and an RTX 3050 graphics card. The software development platform was a Windows 11 64-bit operating system. The entire experiment was implemented using the OpenCV 3.4.2.16 open-source software library, the programming language was Python, and the processing and analysis of shape feature data were performed using Origin 2019 software.

3 Selection of indices for tomato shape detection from top view

The collected top-view tomato images (Figure 5) included two postures with the fruit pedicle downward (Figure 5a) and upward (Figure 5b). For some deformed tomatoes, when the tomato was

placed on the stage with the fruit pedicle upward, the pedicle could not keep the stem in the center of the field of view of the camera. Thus, the shape result of the tomato image collected in this pose differed significantly from the actual shape. In contrast, when the fruit pedicle was downward, the tomato body could be stably maintained in the center of the camera’s field of vision. Therefore, the top-down view of tomatoes with the pedicle downward was selected for the experiment.



a. Pedicle down b. Pedicle up

Figure 5 Top-view images of a tomato

3.1 Roundness

Roundness indicates how close the tomato outline is to a circle. A value closer to one indicates that the tomato outline is closer to a circle. The ratio of the contour area to the square of the perimeter and the minimum circumscribed circle fitting degree are common roundness features^[31,32]. Examining the shape characteristics of the tomato from the top view, revealed that the area ratio of the maximum inscribed circle to the minimum circumscribed circle of the contour accurately reflected the circularity of the contour. Therefore, in this study, roundness, the minimum circumscribed circle fit, and the area ratio of the maximum inscribed circle to minimum circumscribed circle were used to characterize the roundness of the tomato, which were calculated according to the following equations:

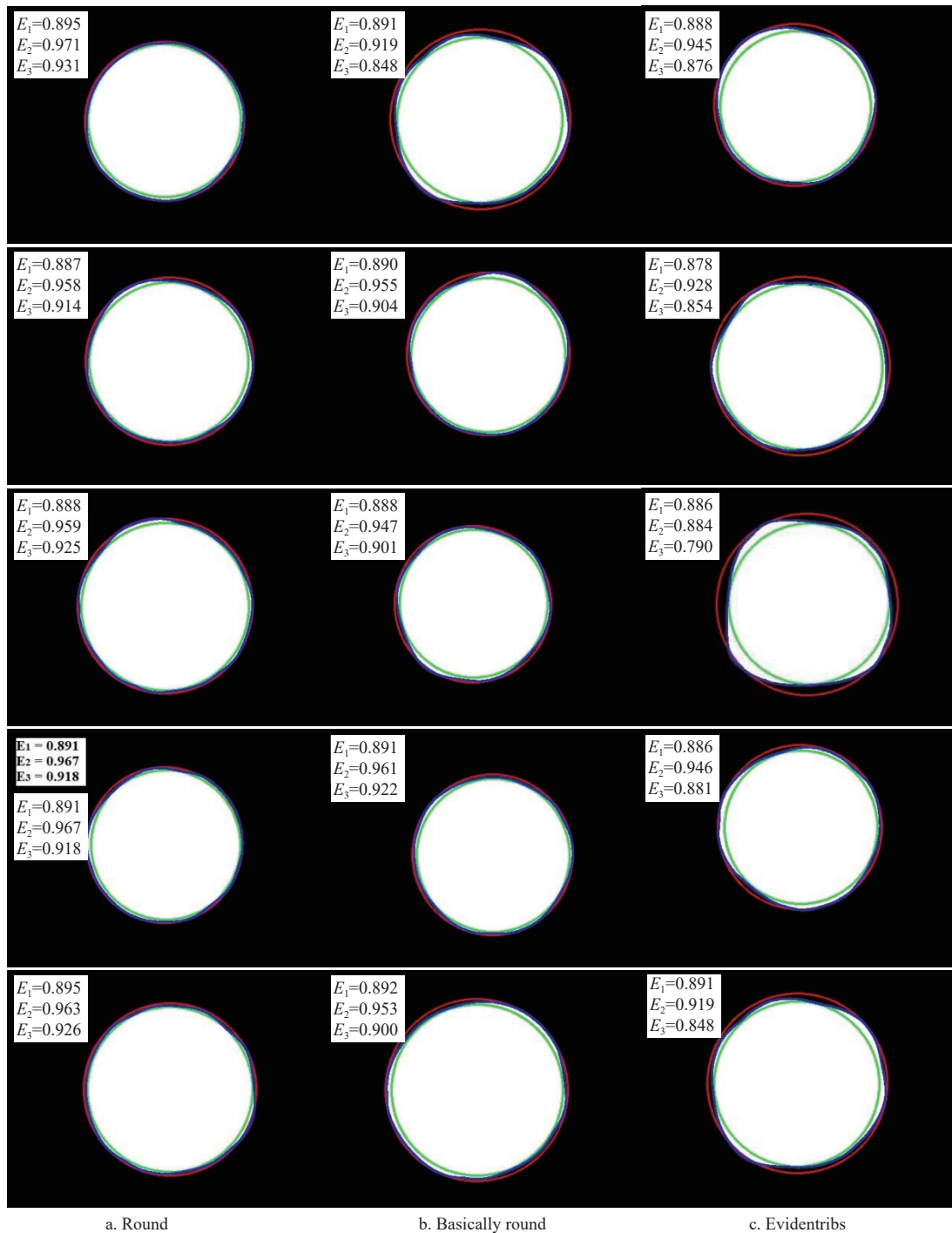
$$E_1 = \frac{4 \times \pi \times A}{C^2} \quad (2)$$

$$E_2 = \frac{A}{\pi \times R_{\min}^2} \quad (3)$$

$$E_3 = \frac{\pi \times R_{\max}^2}{\pi \times R_{\min}^2} \quad (4)$$

where, E_1 , E_2 , and E_3 represent the roundness, the minimum circumscribed circle fit, and the area ratio of the maximum inscribed circle to minimum circumscribed circle respectively; A represents the projected area of the tomato target in the image; C represents the perimeter of the tomato outline, obtained through the `cv2.arcLength()` function; R_{\min} and R_{\max} represent the radii of the minimum circumscribed circle and the maximum inscribed circle, respectively.

Figure 6 shows the differences in roundness among tomatoes with different shapes, where the green circle is the maximum inscribed circle of the tomato, the red circle is the minimum circumscribed circle, and the blue curve is the outline shape of the tomato. The round-tomato contour almost coincided with its maximum inscribed circle and minimum circumscribed circle (Figure 6a). There was a slight gap between the minimum circumscribed circle and the maximum inscribed circle of the round tomato contour (Figure 6b). For tomatoes with evident ribs, the gaps between the contour and the maximum inscribed circle and minimum circumscribed circle were relatively large (Figure 6c). Therefore, it is feasible to judge the roundness of a tomato by the proximity of its contour to its maximum inscribed circle and maximum circumscribed circle.



Note: Images output by Pycharm. E_1 , E_2 , and E_3 represent the roundness, the minimum circumscribed circle fit, and the area ratio of the maximum inscribed circle to the minimum circumscribed circle respectively.

Figure 6 Differences in roundness among tomatoes with different shapes

3.2 Centroid distance

The centroid distance refers to the Euclidean distance from the centroid to the contour point of the tomato and is typically used in the process of calculating the Fourier descriptor. Because of the complex calculation process for the Fourier descriptor (coordinate transformation and Fourier transformation are required), the centroid distance was directly used to describe the tomato shape in this study. Output the contour coordinates of tomatoes through the contour lookup function and calculate the image moments within the third order of the contour. Use the zero-order moment and the first-order moment to calculate the center of mass coordinates. The calculation equations were as follows:

$$x = \frac{m_{10}}{m_{00}} \tag{5}$$

$$y = \frac{m_{01}}{m_{00}} \tag{6}$$

where, x and y represent the center of mass coordinates; m_{10} and m_{01} represent the two first-order moments of the tomato contour; m_{00} represents the zero-order moment. After the centroid and contour coordinates were obtained, the Euclidean distance was calculated with the centroid as the reference point and the coordinates of the edge point of the fruit, and it was normalized as follows:

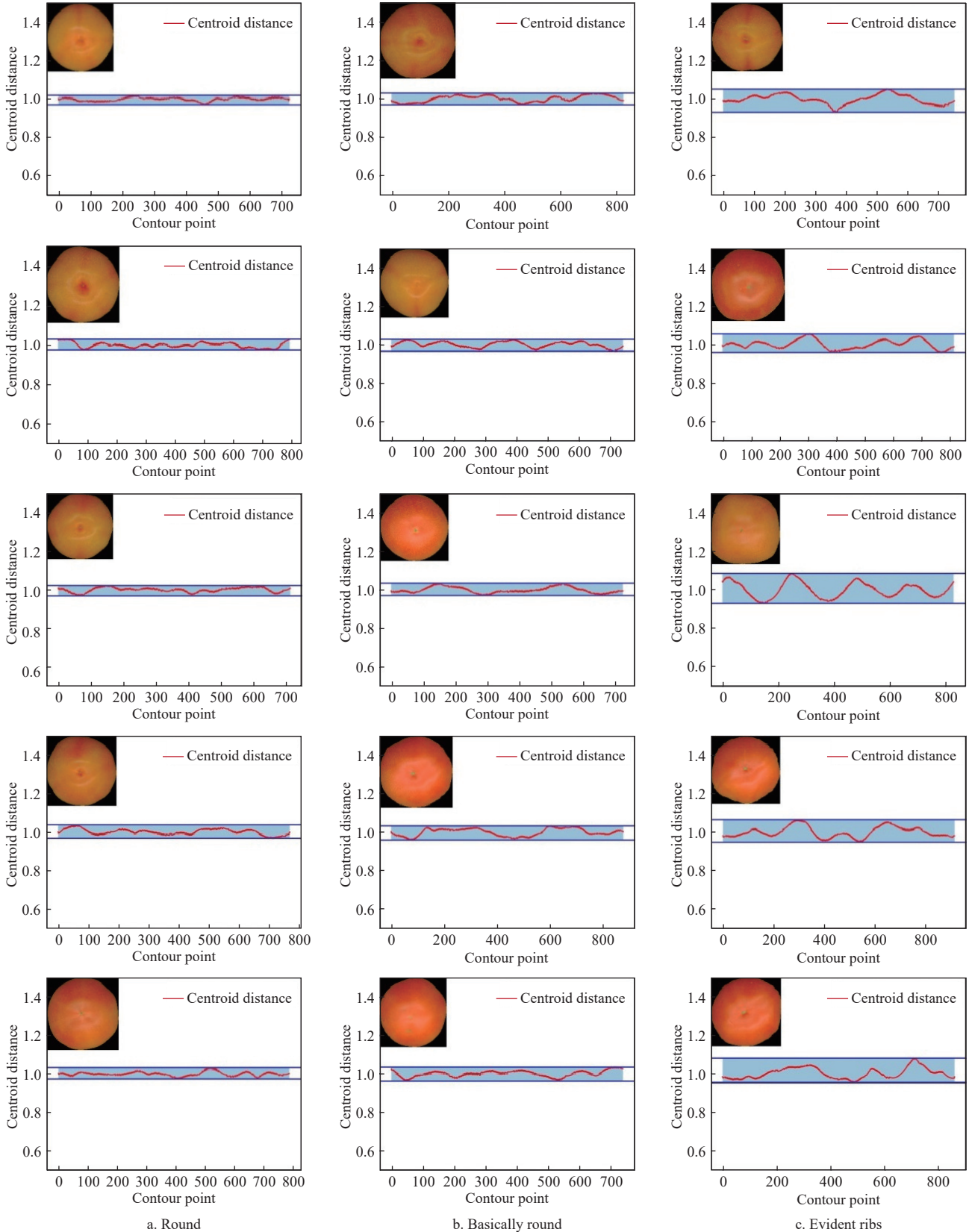
$$d_i = \sqrt{(x_i - x_0)^2 + (y_i - y_0)^2} \tag{7}$$

$$d^* = \frac{d_i}{\frac{1}{N} \sum_{i=1}^N d_i} \quad (8)$$

where, x_0 and y_0 are the horizontal and vertical coordinates of the centroid, respectively; x_i and y_i are the horizontal and vertical

coordinates of the i th point on the contour of the fruit body, respectively; d_i represents the Euclidean distance from the centroid to the i th contour point; N represents the number of tomato contour points; d^* represents the normalized centroid distance.

The normalized centroid-distance curve fluctuates up and down on the line $y=1.0$ (Figure 7). For the round tomatoes, the centroid



Note: Images output by Pycharm. Each column represents a tomato shape, and five representative images were selected for each shape of the tomato.

Figure 7 Centroid distance curves of tomatoes with different shapes

distance has a relatively narrow fluctuation range (0.97, 1.03), that was, the distribution of the centroid-distance data is relatively concentrated (Figure 7a); With an increase in the degree of fruit shape deformation, the fluctuation range of the centroid-distance curve widened (Figures 7b and 7c), the fluctuation range of the centroid distance curve of basically round and obviously ribbed tomatoes was (0.95, 1.04) and (0.93, 1.08), respectively; that was, the degree of data dispersion increased. Thus, the dispersion degree of the centroid distance can reflect changes in tomato shape.

The indicators used for evaluating the data dispersion were the range, mean, standard deviation, and coefficient of variation.

$$x^* = \text{Max}(x) - \text{Min}(x) \quad (9)$$

$$\bar{x} = \frac{1}{N} \sum_{i=1}^N x_i \quad (10)$$

$$\sigma = \sqrt{\frac{1}{N} \sum_{i=1}^N (x_i - \bar{x})^2} \quad (11)$$

$$\text{CV} = \frac{\sigma}{\bar{x}} \times 100\% \quad (12)$$

where, $\text{Max}(x)$ and $\text{Min}(x)$ represent the maximum and minimum values of the Euclidean distance, respectively; x_i represents the Euclidean distance from the i^{th} contour point in the data to the centroid; x^* represents the range of the data; \bar{x} represents the mean; σ represents the standard deviation; CV represents the coefficient of variation. After normalization, the mean value of the Euclidean distance of each tomato was 1, and the standard deviation was proportional to the coefficient of variation. Therefore, the mean and standard deviation were discarded when evaluating the dispersion.

3.3 Other common shape features

To validate the feasibility of the proposed method for tomato shape detection, the maximum transverse diameter and maximum longitudinal diameter of the tomato contour were extracted, and their ratio and eccentricity were calculated as common shape features for comparison.

$$S_z = \frac{L_{\max}}{L_{\min}} \quad (13)$$

$$E_p = 2 \frac{\sqrt{\left(\frac{L_{\max}}{2}\right)^2 - \left(\frac{L_{\min}}{2}\right)^2}}{L_{\max}} \quad (14)$$

where, L_{\max} and L_{\min} represent the maximum transverse and longitudinal diameters of the tomato, respectively; S_z represents the ratio of the maximum longitudinal diameter to the maximum transverse diameter (a value closer to 1 indicates that the tomato shape is closer to a circle); E_p represents the eccentricity of the tomato (a value closer to 0 indicates that the tomato shape is closer to a circle).

3.4 Analysis and comparison of characteristic indicators

In this study, 200 tomatoes with different shapes were used to extract the above seven shape features, and according to the results of manual classification, the indicators suitable for the shape detection of the tomato top view were selected. Figure 8 shows the data distribution diagram and Table 1 lists the data mean of each indicator for the different shape categories. As shown, the mean values of E_1 for different shapes were close and easy to confuse. E_2 differed significantly among the different shape categories, indicating that it can be used for shape classification. The E_3 values

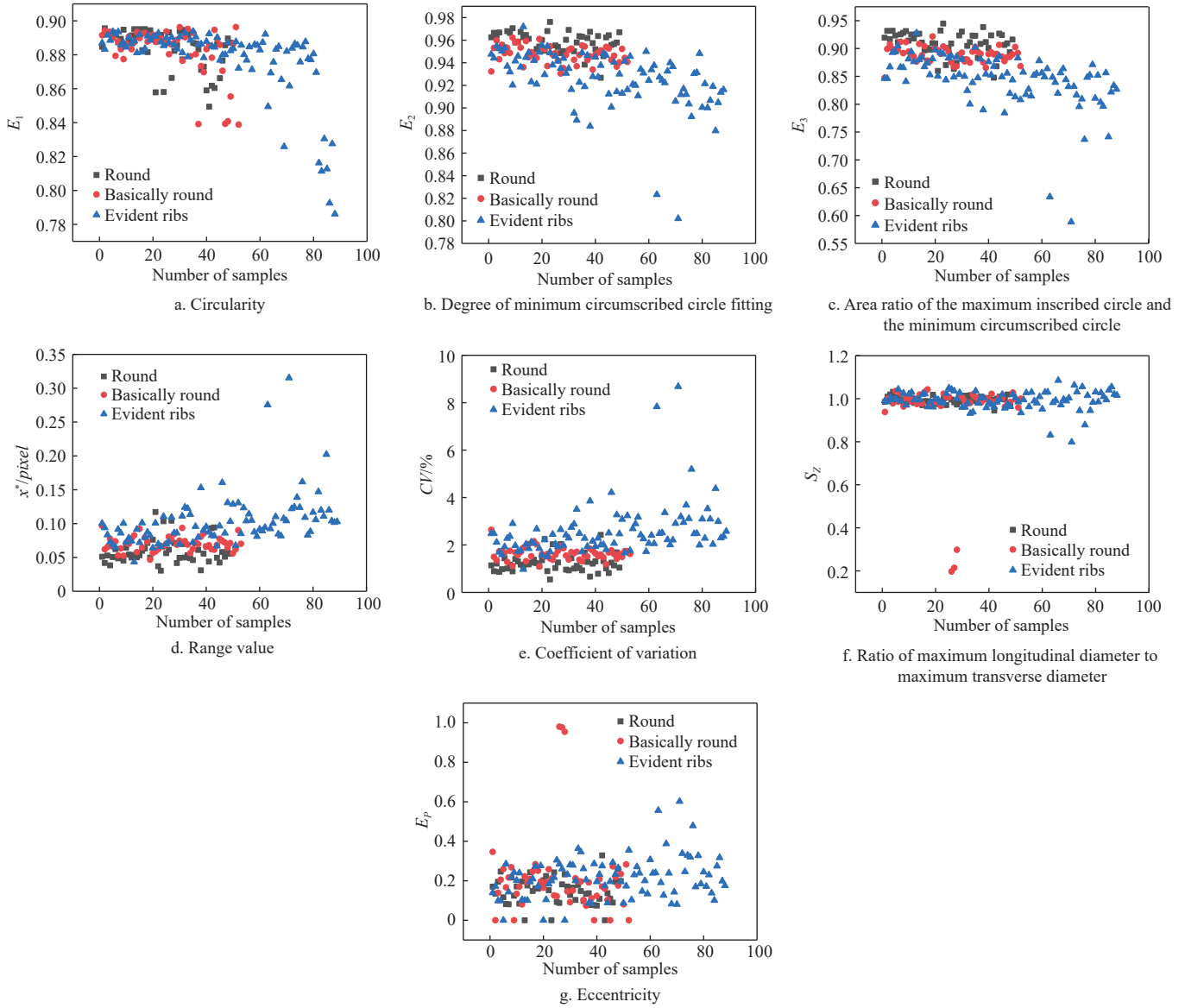
for round tomatoes were mostly >0.910 , for basically round tomatoes were concentrated in the range of (0.879, 0.905), and for tomatoes with evident ribs were <0.880 . The range of the centroid distance for tomatoes in the three shape categories was distributed in the intervals of (0.049, 0.063), (0.062, 0.077), and (0.082, 0.175), respectively. The coefficient of variation for the round tomatoes was $<1.328\%$, for the round tomatoes was between 1.486% and 1.740%, and for tomatoes with evident ribs was $>1.996\%$. For all three shape categories, the average values of range and the coefficient of variation differed significantly, indicating that the method based on the centroid distance can be used to detect the tomato shape. The S_z values for the three shape categories were very close, and their distribution intervals overlapped significantly, making them easy to confuse. The distribution of the eccentricity E_p for the different shapes is highly scattered, and the data points were randomly cross-distributed without a clear law.

After an analysis, the minimum circumscribed circle fitting degree, the area ratio of the maximum inscribed circle to the minimum circumscribed circle, and the range, and variation coefficient of the centroid distance were selected as the characteristic parameters for the shape classification of the tomato top view. The classification thresholds were 0.953 and 0.937, 0.900 and 0.867, 0.064 and 0.087, and 1.426 and 2.099, respectively.

4 Selection of indices for tomato shape detection from side view

The shape description of the tomato from the side view is more complex than that from the top view, because, the shapes of the same tomato observed from different angles may be inconsistent (Figure 9). From the perspective shown in Figure 9a, the tomato shape was evaluated as a symmetric circular shape, whereas the shape of the tomato was distorted from the angle shown in Figure 9b. To comprehensively detect the shape of a tomato, two side images with a difference of 90° in the angles were considered.

The centroid-distance curves obtained from side images of tomatoes with different shapes are shown in Figure 10. The key to determining the shape of the tomato side is to accurately determine the position of the fruit pedicle^[29] because the pedicle is usually located on the fruit axis (central axis). Whether the tomato shape is correct can be judged by determining the position of the pedicle. First, the `cv2.findContours()` function was used to output the tomato contour points, and then the `signal.argrextrema()` function in the SciPy library was used to determine the maximum and minimum values of the centroid distance. According to the shape characteristics of the tomato, the pedicle was determined to be roughly located at the midpoint of the curve. Considering that the central axis of the tomato cannot be completely perpendicular to the central axis of the camera during image acquisition, the shape in the tomato image may have been distorted, that is, the position of the hilum deviates from the midpoint of the contour. Therefore, in this study, the search range of the stem point is set as (length (contour)/5, 4 length (contour)/5), and the minimum point in this range is the centroid distance of the tomato stem point. As shown in Figure 10, the centroid distance curves of both round and oblate tomatoes were “M”-shaped; that is, there were two evident peaks and one deep wave trough (centroid distance of fruit pedicle). The centroid-distance curves of oblong tomatoes had three or more peaks. The two peaks adjacent to the pedicle point in the centroid-distance curve were almost identical for symmetric tomatoes, whereas the values in the distorted-tomato centroid-distance curve were significantly different.



Note: Images output by Origin

Figure 8 Distributions of the roundness parameters for different shapes from the top view

Table 1 Average values for the characteristics of tomatoes with different shapes from the top view

Evaluation indicators		Shape		
		Round	Basically round	Evident ribs
Roundness	E_1	0.884	0.883	0.878
	E_2	0.958	0.948	0.926
	E_3	0.909	0.890	0.845
Centroid distance	$x/pixel$	0.058	0.070	0.103
	$CV/\%$	1.229	1.623	2.575
Other common shape features	S_z	0.996	0.951	0.993
	E_p	0.147	0.213	0.215

Note: E_1 , E_2 , and E_3 represent the roundness, the minimum circumscribed circle fit, and the area ratio of the maximum inscribed circle to minimum circumscribed circle respectively; CV represents the coefficient of variation; S_z represents the ratio of the maximum longitudinal diameter to the maximum transverse diameter; E_p represents the eccentricity of the tomato.

4.1 Symmetry

The side shape of a normal tomato is shown in Figure 10a, where the fruit is approximately circular, the bottom concave area is the position of the fruit pedicle, and the shapes on both sides of the fruit axis are almost symmetric. In this study, the numerical difference between the two peaks (maximum value) of the centroid-distance curve (C_{max}) was used as an index to evaluate the symmetry

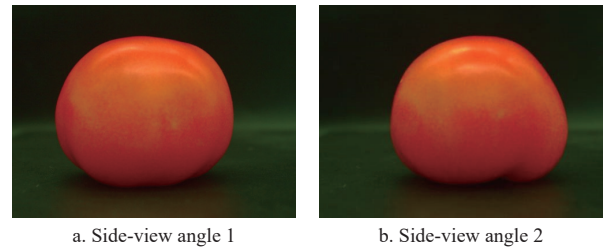


Figure 9 Images of the same tomato from different angles

of the fruit body. The symmetry index was calculated as follows:

$$C_{max} = |\max_1 - \max_2| \tag{15}$$

where, C_{max} represents the difference between the two maxima adjacent to the fruit pedicle in the centroid-distance curve; \max_1 and \max_2 represent the two maximum values of centroid distances adjacent to the fruit pedicle at the centroid distance. A smaller value of C_{max} , corresponds to a more symmetric shape of the tomato side.

4.2 Oblong-oblate degree

The oblong-oblate degree represents the degree to which the shape of the side of the tomato deviates from a circle. In this study, the difference between the minimum centroid distance corresponding

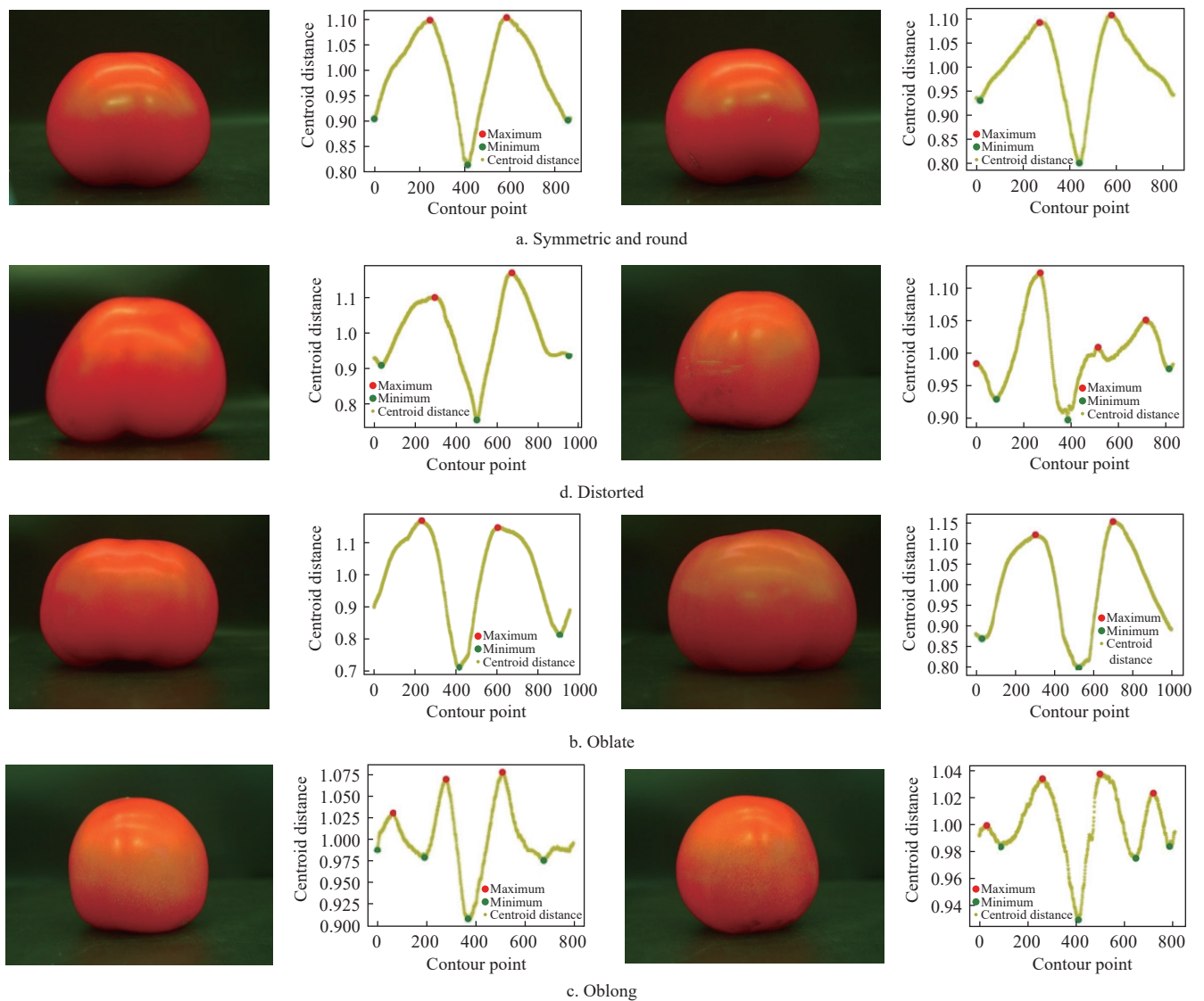


Figure 10 Euclidean distance curves of tomatoes with different shapes

to the fruit pedicle and its adjacent maximum (C_{\min} for short) was used to measure the oblong–oblate degree of the side shape of the tomato. It was calculated as follows:

$$C_{\min} = |\max - \min| \tag{16}$$

where, C_{\min} represents the difference between the maximum and minimum centroid distances; min represents the minimum centroid distance corresponding to the fruit pedicle; max represents the maximum centroid distance adjacent to the fruit pedicle.

4.3 Other common shape features

The ratio of the longitudinal diameter to the transverse diameter is a commonly used index for evaluating the shapes of mangoes and other fruits^[33], but it is not used to evaluate the shapes of tomatoes. In this study, the minimum circumscribed rectangle (E_c) was used to measure the transverse and longitudinal diameters of tomatoes, and their ratio (length-width ratio, S_c) was calculated to evaluate the length and flatness of the tomato shape. In addition, the minimum circumscribed circle fitting degree of the side profile was extracted and used to evaluate the circularity of the side of the tomato.

$$s_c = \frac{H}{W} \tag{17}$$

$$E_c = \frac{A_c}{\pi R_{\min}^2} \tag{18}$$

where, H and W represent the longitudinal and transverse diameters

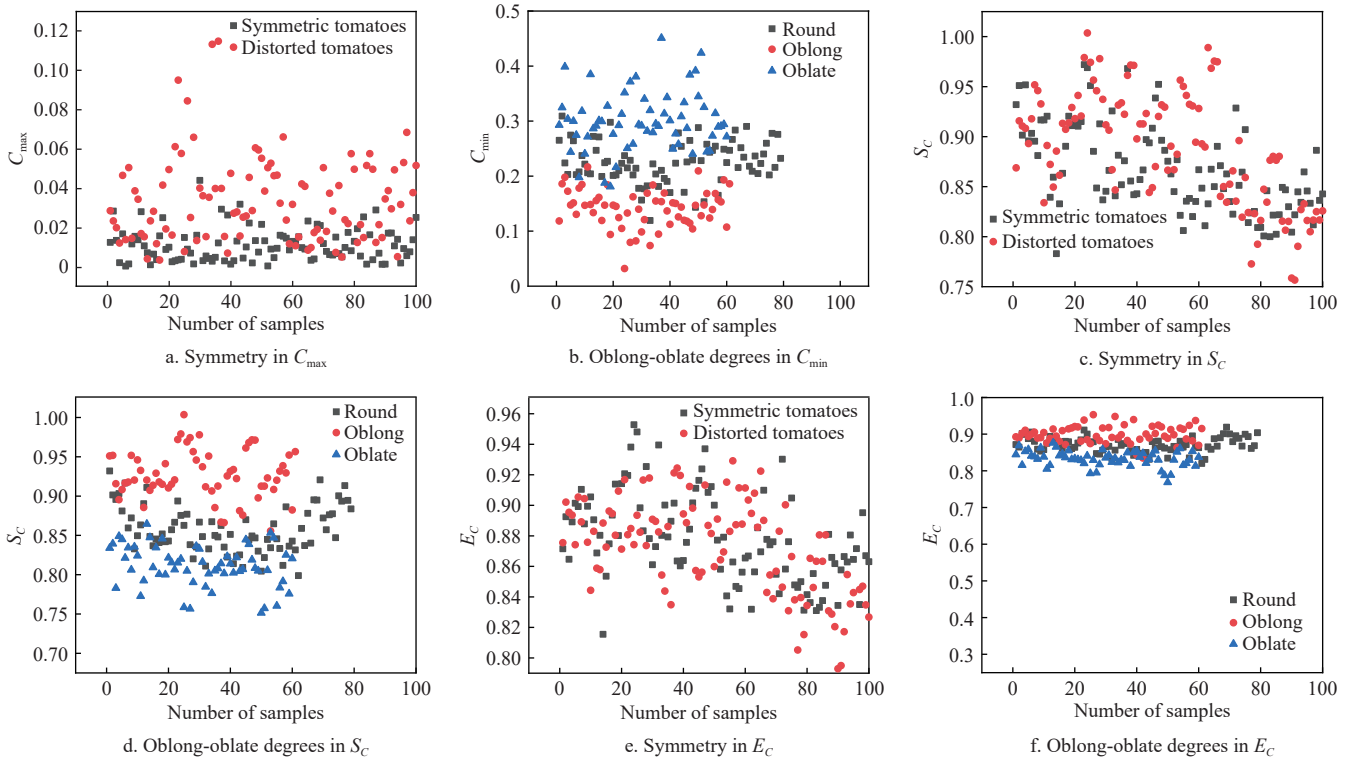
of the tomato, respectively; A_c represents the projected area of the side profile of the tomato; S_c and E_c represent the ratio of the longitudinal diameter to the transverse diameter and the fitting degree of the minimum circumscribed circle on the tomato side, respectively.

4.4 Analysis and comparison of characteristic indicators

The centroid distance, the ratio of the longitudinal diameter to the transverse diameter, and the minimum circumscribed circle fitting degree were extracted from 200 tomato side-view images collected for different shapes. According to the artificial judgment results for the tomato-side shape, the feature index suitable for shape detection of the side view was identified. Figure 11 shows the data distribution diagram of each index for the different shape categories, and Table 2 lists the average values of the indices for the different shape categories. The C_{\max} values of the symmetric tomatoes were <0.02 , and most of the C_{\max} values for tomatoes with evident distortions were >0.02 . A C_{\min} data partition for tomatoes with differences in length and flatness was evident. The C_{\min} values for oblong tomatoes were concentrated between 0.15 and 0.20, the round tomatoes were concentrated between 0.20 and 0.25, and for oblate tomatoes were >0.25 . The mean S_c values differed significantly between the symmetric and distorted tomatoes, but in both cases, the distribution of data points was scattered, without evident regularity. S_c and E_c exhibited good classification effects

for judging the oblong and oblate tomatoes from the side view. Compared with the results of the manual classification, the S_C values for oblate, round, and oblong tomatoes were (0.722, 0.834),

(0.835, 0.902), and (0.903, $+\infty$), respectively, and the E_C data points were distributed in the ranges of (0.734, 0.846), (0.861, 0.887), and (0.886, 0.953), respectively.



Note: Images output by Origin

Figure 11 Data distribution of characteristic parameters for different shapes from the side view

Table 2 Average values for the characteristics of tomatoes with different shapes from the side view

Shape	Detection method	Detection method		
		Centroid distance	S_C	E_C
Symmetry	Symmetric	0.011	0.873	0.881
	Crooked	0.033	0.901	0.880
Oblong-oblate degree	Oblate	0.268	0.808	0.823
	Round	0.202	0.859	0.872
	Oblong	0.125	0.924	0.898

In summary, the C_{max} index of the centroid distance was selected for classifying symmetric and distorted tomatoes, and the classification threshold was set as 0.022. S_C , E_C , and C_{min} were used to distinguish round, oblong, and oblate tomatoes, and the classification thresholds were 0.834 and 0.892, 0.846 and 0.886, and 0.164 and 0.235, respectively.

5 Research on tomato fruit shape grading from different views

After the classification thresholds were determined, the extracted shape features were used to analyze the top and side views of 100 tomatoes with different shapes, and the overall shape of the tomato was determined by the shape discrimination results of multiple views.

5.1 Tomato fruit shape classification from top view

The fitting degree of the minimum circumscribed circle, the area ratio of the maximum inscribed circle to the minimum circumscribed circle, and the range value, and variation coefficient of the centroid distance were used as shape classification indices to

detect the shape of the tomato from the top view, and the results are shown in Figure 12. Where, the numbers 1, 2, and 3 on the vertical axes represent three categories: round, basically round, and evident ribs, respectively. As shown, the shape-detection method based on the minimum circumscribed circle fitting degree had the lowest detection accuracy among the methods tested (66%), it identified some tomatoes with round shapes and evident ribs, but the detection accuracy for basically round tomatoes was very low. The method using the area ratio of the maximum inscribed circle to the minimum circumscribed circle achieved a detection accuracy of 84%, indicating that this method can replace the commonly used circularity index for tomato shape detection. The classification method using the range of the centroid distance had a low accuracy of 77%, and most of the misidentified tomatoes were round shapes. The shape detection method using the coefficient of variation achieved the highest accuracy (94%), it accurately identified normal deformed, and slightly deformed tomatoes; thus, it can satisfy the requirements of tomato shape classification in the actual production and packaging process.

5.2 Tomato fruit shape classification from side view

The shapes of the tomatoes from the side view were classified using three features: the ratio of the longitudinal diameter to the transverse diameter, minimum circumscribed circle fitting degree, and centroid distance. The results are shown in Figure 13. In Figure 13a, the numbers 0 and 1 on the vertical axes represent symmetric and distorted shapes, respectively, and in Figure 13b, the numbers 0, 1, and 2 represent oblong, round, and oblate, respectively. The symmetry detection method based on the centroid distance achieved an accuracy of 91.91%, indicating that it can satisfy the requirements for the classification of tomato shapes in

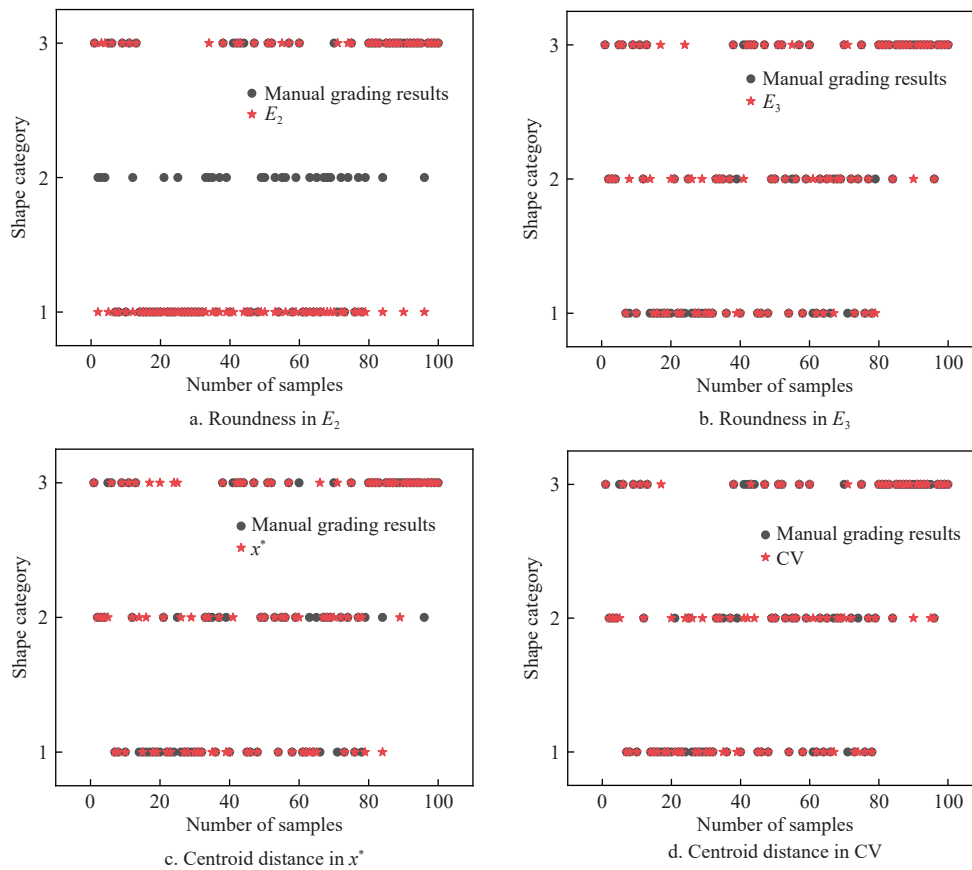


Figure 12 Shape-detection results for the top view

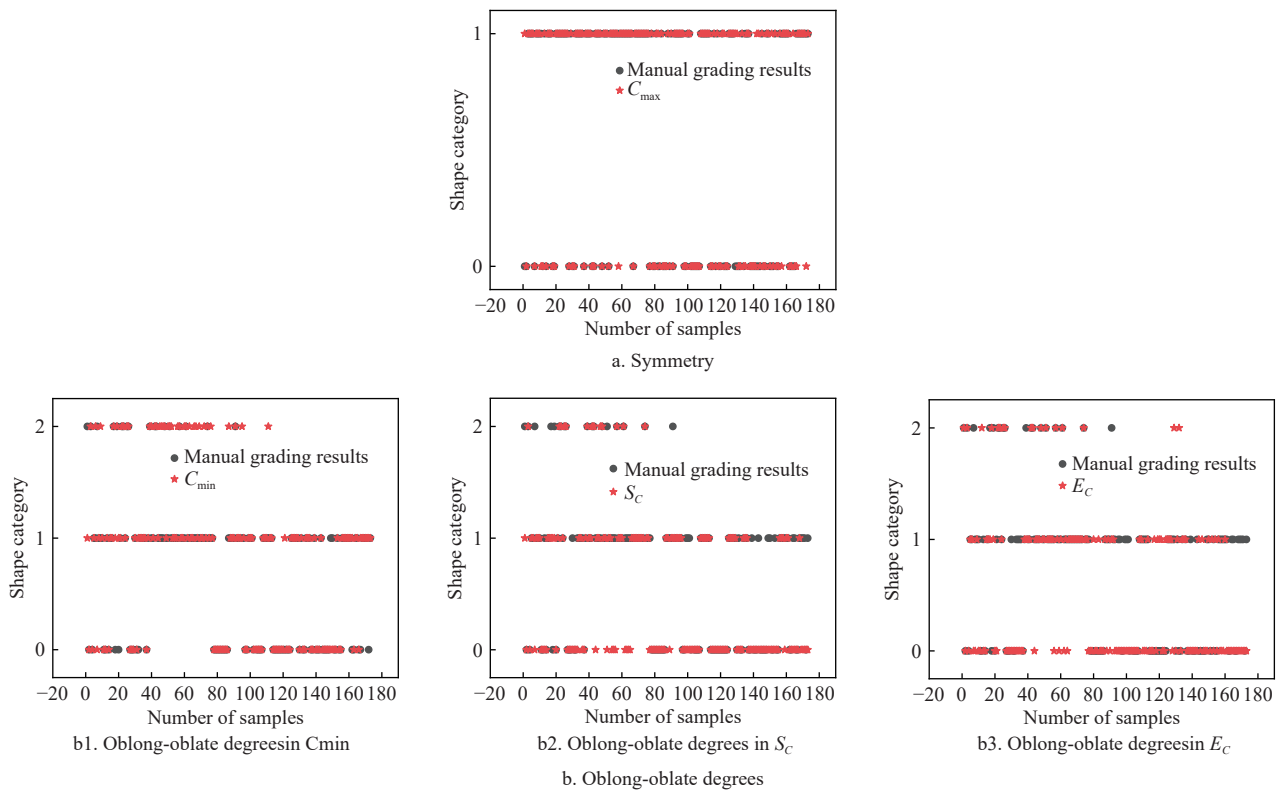


Figure 13 Side-view shape-detection results

the actual production process. The accuracy for detecting oblong-oblate tomatoes according to the centroid distance was 85.08%, indicating that the proposed centroid-distance method can accurately identify the tomato-side shape. The shape-detection methods based on the ratio of the longitudinal diameter to the

transverse diameter and the minimum circumscribed circle fitting degree of the side profile had detection accuracies of 77.46% and 64.16% for the shape of the tomato side, respectively, which were significantly lower than that of the centroid-distance method. The misclassification of tomatoes in the detection process is attributed to

the change in the image-acquisition angle: when the tomato in the image protruded forward (tilted) or the fruit pedicle was located at the edge of the tomato image, the probability of computer misclassification of the tomato shape increased.

5.3 Multi-view fusion

After obtaining the top- and side-view tomato shape results, they were integrated to perform an overall shape evaluation of the tomato. Based on the shape results for the top view, the shape results for the side views with a difference of 90° in the angles were considered separately. If any angle in the side image was distorted or noncircular (oblong or oblate), the tomato was classified as the poor level.

According to the shape determination method for a single tomato fruit shown in Figure 14, the shape determination of 100 tomatoes was performed for validation, and the results are presented in Figure 14a. As shown, the method of identifying the tomato shape only from the top-view or side-view images was inconsistent. As can be seen from Figure 14b, when grading tomato shapes from top and side view, the number of misclassifications of special-grade tomatoes were 7 and 3, that is, the detection accuracies for special-grade tomatoes were 78.79% and 91.67%; the number of misclassification of unqualified tomatoes were 3 and 5, that is, the detection accuracies for unqualified tomatoes were 90.29% and 86.84%; and the number of misclassification of unqualified tomatoes were 13 and 7, that is, the detection accuracies for first-grade tomatoes were 75.61% and 85.37%. The classification accuracy of the multi-view shape-result integration method was 96%. The number of wrong grades of super-grade and first-grade tomatoes is 4 and 3, respectively, which indicates that detection accuracies for the different shape categories were all $>80\%$, and the detection accuracy for unqualified tomatoes (deformed) was 100%, the number of wrong grades is 0. Misidentification occurred mainly for special tomatoes and first-grade tomatoes. This may be because when judging a tomato with confusing shape characteristics of individual side views, the computer performed the grading strictly according to the set classification threshold. However, there was a degree of subjectivity in the manual grading, which led to inconsistencies between the computer and manual grading results for individual tomatoes.

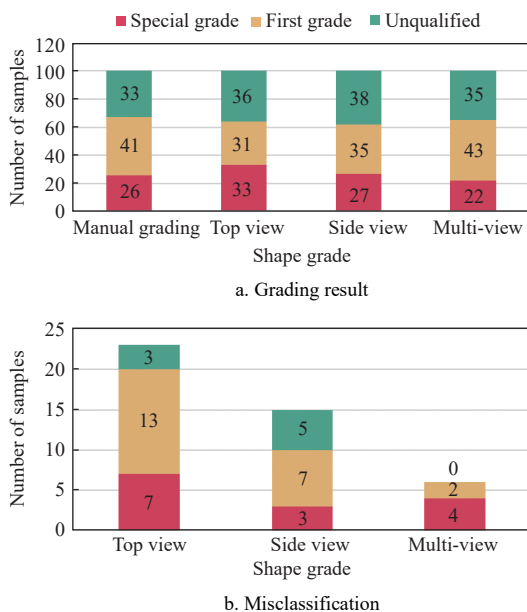


Figure 14 Tomato shape detection results

6 Conclusions

Machine vision was used to detect the shapes of tomatoes from top and side views. The A-component map in the LAB color model was used to perform Otsu threshold segmentation, and the complete tomato target was extracted for feature extraction and shape grading. Finally, the shape judgment results from multiple perspectives were integrated to perform an overall shape evaluation of the tomatoes.

1) For shape detection from the top view, three new indicators were established: the range value and the coefficient of variation based on the centroid distance of the contour and the area ratio of the maximum inscribed circle to the minimum circumscribed circle. There are four commonly used indicators: contour roundness, minimum circumscribed circle fitting degree, eccentricity, and ratio of the maximum longitudinal diameter to the maximum transverse diameter. Through data analysis, three indicators (roundness, eccentricity, and ratio of the maximum longitudinal diameter to the maximum transverse diameter) were discarded, and the minimum circumscribed circle fitting degree, area ratio of maximum inscribed circle to minimum circumscribed circle, and range value and variation of the centroid distance were used. The shape grading accuracies for these indicators are 66%, 84%, 77%, and 94%, respectively;

2) For shape detection from the side view, an evaluation index based on the contour centroid distance curve shape was developed, and grading accuracies of 91.91% and 85.08% were achieved for the symmetry and oblong-oblate degree, respectively. The classification accuracies for the ratio of the longitudinal diameter to the transverse diameter and the fitting degree of the minimum circumscribed circle of the side contour were 77.46% and 64.16%, respectively;

3) A shape-evaluation method for multi-view shape-result fusion was developed, which predominantly uses the top view and is supplemented by the side view. The classification accuracy reached 96%, with the highest identification accuracy of unqualified tomatoes.

In this study, tomato shapes were classified from two perspectives: top and side view. The classification results for the two perspectives were combined to realize omnidirectional and multi-perspective shape discrimination of tomatoes, and the proposed method is suitable for assembly-line production and packaging of factory tomatoes. The tomato images in this study were collected under the condition of static and single sample, and the quality detection of dynamic and multi-copy tomato sequence images can be further explored in the future, so as to achieve pipelined tomato online grading.

Acknowledgements

This work was financially supported by the Beijing Nova Program (Grant No. 2023141), Yunnan Key Research and Development Program (Grant No. 202202AE090066), and the Project of Beijing Academy of Agricultural Sciences (Grant No. YXQN202304)

[References]

- [1] Zhang H. According to the current situation of the global tomato industry, there is still a big gap between China's tomato production and foreign countries. China Economic Information Network. Available: <https://www.huaon.com/channel/trend/729400.html>. Accessed on [2021-07-06]. (in Chinese)

- [2] NYT940-2006. Grades and specifications of tomatoes. 2006; 8p. (in Chinese)
- [3] Costa C, Antonucci F, Pallottino F, Aguzzi J, Sun D W, Menesatti P. Shape analysis of agricultural products: a review of recent research advances and potential application to computer vision. *Food and Bioprocess Technology*, 2011; 4(5): 673–692.
- [4] Lu H S, Wang F J, Liu XL, Wu Y Y. Rapid assessment of tomato ripeness using visible/near-infrared spectroscopy and machine vision. *Food Analytical Methods*, 2017; 10(6): 1721–1726.
- [5] Wang A C, Fu X P, Xie L J. Application of visible/near-infrared spectroscopy combined with machine vision technique to evaluate the ripeness of melons (*Cucumis melo* L.). *Food Analytical Methods*, 2015; 8(6): 1403–1412.
- [6] Sarkar T, Mukherjee A, Chatterjee K, Ermolaev V, Piotrovsky D, Vlasova K, et al. Edge detection aided geometrical shape analysis of Indian gooseberry (*Phyllanthus emblica*) for freshness classification. *Food Analytical Methods*, 2022; 15(6): 1490–1507.
- [7] Saglam C, Cetin N. Prediction of pistachio (*Pistacia vera* L.) mass based on shape and size attributes by using machine learning algorithms. *Food Analytical Methods*, 2022; 15(3): 739–750.
- [8] Sun K, Li Y, Peng J, Tu K, Pan L Q. Surface gloss evaluation of apples based on computer vision and support vector machine method. *Food Analytical Methods*, 2017; 10(8): 2800–2806.
- [9] Bhargava A, Barisal A. Automatic detection and grading of multiple fruits by machine learning. *Food Analytical Methods*, 2020; 13(3): 751–761.
- [10] Sun D-W, Costa C, Menesatti P. Advantages of using quantitative shape descriptors in protocols for plant cultivar and postharvest product quality assessment. *Food and Bioprocess Technology*, 2011; 5(1): 1–2.
- [11] Cai Y. Research on quality inspection and grading of tomatoes based on machine vision. Master dissertation. Guangzhou: Sun Yat-sen University, 2010; 83p. (in Chinese)
- [12] Wang H Z. Image recognition method of tomato appearance characteristics. Master dissertation. Yangling: Northwest A&F University, 2018; 52p. (in Chinese)
- [13] Arjenaki O O, Moghaddam P A, Motlagh A M. Tomato sorting based on maturity, surface defects and shape by using of machine vision system. In: Proceedings of the CIGR-AGENG, 2012.
- [14] Zhang Q, Zuo X J, Lin G C, Sun Y H. Image feature extraction and online grading method for weight and shape of strawberry. *Journal of System Simulation*, 2019; 31(1): 7–15. (in Chinese)
- [15] Wang J T, Mu H T. An improved Hu moment of tomato shape feature extraction based on FFT. *Machinery Design & Manufacture*, 2019; 5: 228–231.
- [16] Ying Y B, Gui J S, Rao X Q. Fruit shape classification based on Zernike moments. *Journal of Jiangsu University (Natural Science Edition)*, 2007; 28(1): 1–3, 67. (in Chinese)
- [17] Hao M, Ma S S, Hao X D. Potato shape detection based on Zernike moments. *Transactions of the CSAE*, 2010; 26(2): 347–350. (in Chinese)
- [18] Gui J S, Zhang Q, Hao L, Bao X A. Apple shape classification method based on wavelet moment. *Sensors & Transducers Journal*, 2014; 178(9): 182–187.
- [19] Li C Y, Cao Q X. Extraction method of shape feature for vegetables based on depth image. *Transactions of the CSAM*, 2012; 43(S1): 242–245. (in Chinese)
- [20] Yuan L, Tu X Y, Ju G, Liu Z B, Wu J Q. Tomato real-time classification based on machine vision detection system design. *Journal of Xinjiang University (Natural Science Edition)*, 2017; 34(1): 11–16. (in Chinese)
- [21] Liu L, Li Z K, Lan Y F, Shi Y G, Cui Y J. Design of a tomato classifier based on machine vision. *PLoS ONE*, 2019; 14(7): e0219803.
- [22] Yao Y F, Liu F, Zhang H D, Li C, Zhou H J, Wang M. Research on octagon color and fruit shape recognition based on machine vision. *Journal of Agricultural Science and Technology*, 2021; 23(11): 110–120. (in Chinese)
- [23] Antonucci F, Costa C, Pallottino F, Paglia G, Rimatori V, De Giorgio D, Menesatti. Quantitative method for shape description of almond cultivars (*Prunus amygdalus* Batsch). *Food and Bioprocess Technology*, 2012; 5(2): 768–785.
- [24] Ishikawa T, Hayashi A, Nagamatsu S, Kyutoku Y, Dan I, Wada T, et al. Classification of strawberry fruit shape by machine learning. *ISPRS - The International Archives of the Photogrammetry, Remote Sensing and Spatial Information Sciences*, 2018; 42(2): 463–470.
- [25] Tigistu T, Abebe G. Classification of rose flowers based on Fourier descriptors and color moments. *Multimedia Tools and Applications*, 2021; 80(30): 36143–36157.
- [26] Xiao A L, Pan B. Identification of the shape of Chinese date based on Labelling method and extremum of polar radius. *Journal of Agricultural Mechanization Research*, 2015; 37(7): 61–65. (in Chinese)
- [27] Pei Y K, Ye J M, Jiang Y C, Lian M Y, Han X X, Gu Y. The cherry shape and size detection technology based on machine vision. *The Food Industry*, 2020; 41(8): 199–202. (in Chinese)
- [28] Li Y, Shen J, Xie H, Gao G Y, Liu J X, Liu J. Detection and grading method of pomelo shape based on contour coordinate transformation and fitting. *Smart Agriculture*, 2021; 3(1): 86–95. (in Chinese)
- [29] Guo H. Research on pummelo quality detection based on machine vision. PhD dissertation. Beijing: China Agricultural University, 2015; 133p. (in Chinese)
- [30] DB11/T 907.1-2012. Identification experiment code for vegetable varieties Part 1: Solanaceous fruits. 2012.
- [31] Yin R, Gao J, Meng G F, Pan Y Y. A method of tomato shape classification with the application of circularity. *Journal of Changshu Institute of Technology*, 2013; 27(4): 100–103. (in Chinese)
- [32] Li J, Wu C P, Liu M H, Chen J Y, Zheng J H, Zhang Y F, et al. Detection of shape characteristics of kiwifruit based on hyperspectral imaging technology. *Spectroscopy and Spectral Analysis*, 2020; 40(8): 2564–2570. (in Chinese)
- [33] Mon T, ZarAung N. Vision based volume estimation method for automatic mango grading system. *Biosystems Engineering*, 2020; 198: 338–349.